

A low energy differential Cerenkov Counter

J. D. Fox

April 1972

Collider Accelerator Department
Brookhaven National Laboratory

U.S. Department of Energy

USDOE Office of Science (SC)

Notice: This technical note has been authored by employees of Brookhaven Science Associates, LLC under Contract No.AT(30-1)-16 with the U.S. Department of Energy. The publisher by accepting the technical note for publication acknowledges that the United States Government retains a non-exclusive, paid-up, irrevocable, world-wide license to publish or reproduce the published form of this technical note, or allow others to do so, for United States Government purposes.

DISCLAIMER

This report was prepared as an account of work sponsored by an agency of the United States Government. Neither the United States Government nor any agency thereof, nor any of their employees, nor any of their contractors, subcontractors, or their employees, makes any warranty, express or implied, or assumes any legal liability or responsibility for the accuracy, completeness, or any third party's use or the results of such use of any information, apparatus, product, or process disclosed, or represents that its use would not infringe privately owned rights. Reference herein to any specific commercial product, process, or service by trade name, trademark, manufacturer, or otherwise, does not necessarily constitute or imply its endorsement, recommendation, or favoring by the United States Government or any agency thereof or its contractors or subcontractors. The views and opinions of authors expressed herein do not necessarily state or reflect those of the United States Government or any agency thereof.

BROOKHAVEN NATIONAL LABORATORY
Associated Universities, Inc.
Upton, New York

EP&S DIVISION TECHNICAL NOTE

No. 47

John Fox

April 13, 1972

A LOW ENERGY DIFFERENTIAL CERENKOV COUNTER

Introduction

The low energy separated beam (LESB) at the AGS is an electrostatically separated beam from target station C with momentum up to about 1.2 GeV/c. Because there is only one stage of separation, the purity of the beam is rather low, and a counter system with good rejection is needed to identify K's and \bar{p} 's from the pion background. The distance between the mass slit and the final focus can be as short as 195" depending on where the final focus is placed; this distance is sufficient to identify protons by time-of-flight techniques in the momentum range of the beam, but identification of K's is marginal. To identify K's a counter system with good rejection of both pions and protons is needed.

Differential using solid or liquid radiators have been developed by several groups ⁽¹⁾⁽²⁾. These depend on the angle of the Cerenkov light to discriminate between π 's and K's and require a fairly well-collimated beam. Because the LESB is not at all well-collimated but is sharply converging at the final focus, the extreme rays converging at $\pm 5^\circ$, these conventional differential counters would not work in this beam. The usual tactic when confronted with a non-parallel beam is to resort to threshold counters. A threshold counter is difficult in this application for several reasons, (1) the refractive index needed to give light from pions and not from K's is about 1.1; this is a difficult index to obtain with either gas or liquid, (2) the counting rates of an anti counter would be high if it were counting pions while the rejection would have to be very good because of the low beam purity, (3) in a positive beam the protons, which are about as numerous as

the pions, would have to also be rejected with good efficiency.

A differential counter, therefore, appears to be dictated. One thing that makes the problem simpler is that the difference in velocity between pions and K's is relatively large compared to the difference available at higher momenta. The basic idea of the counter described here was first used by Fitch in 1956. (3) (4) The idea appears to be well known, but few descriptions of such counters have appeared in the literature. A radiator is selected with a refractive index sufficiently high that both pions and K's make Cerenkov light but the pion light is emitted at such a large angle that it is totally internally reflected. The phototubes, placed outside the radiator, see only the light that escapes. The protons are below the threshold for Cerenkov light emission. The counter described here is a modification of the Fitch idea with improvements so that (a) a non-parallel beam can be used (b) the proton light can be rejected even when it occurs.

Theory

A particle of velocity βc travelling through material of refractive index n emits Cerenkov light in a cone of angle θ' given by the well known formula

$$(1) \quad \cos \theta' = 1/n\beta \quad n\beta > 1$$

If this Cerenkov light now emerges through a surface perpendicular to the beam axis into a medium of refractive index $n=1$, the angle of the refracted light cone, θ , is defined by the equation

$$(2) \quad \sin \theta = \sqrt{n^2 - 1/\beta^2}$$

When $\sin \theta > 1$ from equation (2) it means that the light is totally reflected and no Cerenkov light can get out of the radiator. The range of β for which light will emerge from the cell is, therefore, defined by

$$(3) \quad 1/n < \beta < 1/\sqrt{n^2 - 1}$$

The refractive index is not a constant, but varies with wave length; it can be fit to an expression of the form

$$(4) \quad n(\lambda) = A / \sqrt{1/\lambda_0^2 - 1/\lambda^2}$$

where the constants A and λ_0 can be found by comparison with refractive indexes at known wavelengths. The values used in this study are given in Table I.

TABLE I

<u>Material</u>	<u>A</u>	<u>λ_0</u>
Lucite ^{crystal}	18.724	.0788 μ
Fuzed Quartz	20.985	.0690 μ

The variation of n with λ is important since, as we shall see, the short wavelengths contribute most of the light.

The number of protons of Cerenkov light per cm of track length in the radiator can be written (5).

$$dN/d\omega = \alpha \sin^2 \theta' / c$$

where $\alpha \approx 1/137$ is the fine structure constant. Substituting from eq (1) and expressing the number of protons as a function of wavelength we get

$$(5) \quad dN/d\lambda = 458.6 (1 - (1/n\beta)^2) / \lambda^2$$

where λ is expressed in microns (1 micron = 10^{-4} cm). To get the number of effective photons we integrate the right hand side of equation (5) over the quantum efficiency function of the phototube $\eta_{pt}(\lambda)$, and fold in the transmission efficiency η_{trans} and collection efficiency η_{coll} thus

$$(6) \quad N_Y = 458.6 \int_{\lambda_{min}}^{\lambda_{max}} (1 - (1/n\beta)^2) \lambda^2 \eta_{pt}(\lambda) \eta_{trans}(\lambda) \eta_{coll}(\lambda) d\lambda$$

where $\eta_{pt}(\lambda)$ is obtained from the manufacturers published data. Since the tubes used in this experiment had glass windows, it is assumed that there is no additional correction needed for the transmission of the radiator, which was UVT lucite or fuzed quartz. λ_{min} and λ_{max} are chosen to include the effective limits of η_{pt} .

$\eta_{trans}(\lambda)$ can be evaluated knowing that the fraction of light reflected is given by the Fresnel formula $R(\lambda) = \tan^2(\theta - \theta') / \tan^2(\theta + \theta')$ (for Cerenkov light the \vec{E} vector is in the plane of reflection)

Then, the fraction of light emerging from the radiator

$$(7) \quad \eta_{trans} = 1 - R(\lambda) = 4 / (s + 1/s + 2)$$

where $s = n \cos \theta / \cos \theta'$

$\eta_c(\lambda)$, the collection efficiency depends, in general on the angle of the light after escaping from the radiator and thus on refractive index and β . In the design of this counter a specular reflector was placed a distance g in front of the radiator of thickness l . The reflector enhances light

collection for sufficiently steep angles of emergence but for shallow angles the light is redirected into the radiator and lost. The geometry of the counter is shown in Fig. 1. In the case shown, the Cerenkov light is being partially reabsorbed. Light from the back of the radiator is being collected, while light from the front is lost. Let y_i be the intersection of the i th ray with the plane of the front of the cell. Then

$$\begin{aligned} y_1 &= 2g \tan \theta && \text{from the front of the cell} \\ y_2 &= y_1 + \ell \tan \theta' && \text{from the back of the cell} \end{aligned}$$

Let r be the radius of the cylindrical cell. Then for a particle trajectory on the axis of the cylinder

$$(8) \quad \begin{aligned} \eta_{(c)} &= 1.0 \text{ for } y_1 > r \\ \eta_{(c)} &= 0.0 \text{ for } y_2 < r \\ \eta_c &= (y_2 - r)/(y_2 - y_1) \text{ for } y_1 < r < y_2 \end{aligned}$$

For off center particle trajectories the rays will start closer than Ω to some phototubes and further than Ω from others. Equation (8) seems to be a reasonable approximation for the average collection efficiency. It should also be expected that the true light collection efficiency will be substantially less than one even for the case where $y_1 > r$ owing to light that strikes gaps between the tubes, less than 100% reflection at the mirror, etc. Equation 8 should therefore be regarded as giving a qualitative picture rather than an absolute number.

The expected number of photons is obtained by integrating numerically the quantities in Equation 6. Figure 2 shows how some of these quantities vary with λ . It can be seen that the most important part of the photon spectrum comes from the invisible ultraviolet, and calculations using $n(\lambda)$ from the sodium D line would be most inaccurate. Figure 3 and Figure 4 shows the total photons as a function of momentum for UVT lucite and fused quartz respectively. The dotted line shows the shape that would be obtained if gap, g , were larger. The small g helps separate the proton and K peaks in the region of 1 GeV, particularly for the fused quartz radiator where there would be a considerable contribution from protons if the proton light were not redirected back into the cell by the reflector.

Design of Counter

An exploded drawing of the counter is shown in Fig. 5. The frame of the pillbox is made of heavy aluminum. The front and back plates are made

thin 1/16", aluminum and are held on by electrical tape. Most of the material in the beam is in the cell itself, which is 1" thick ultraviolet transmitting (UVT) plastic (8): The beam goes through about 2.5 gm. of plastic and .85 gm. of aluminum. The specular reflector is made from heavy aluminum foil glued to a spacer made of styrofoam. The polished face of the cell is spherical with a radius such that the focus of the beam is at the center of this sphere. Thus, even though the beam has an angular divergence of $\pm 5^\circ$ at the extreme, all particle trajectories are perpendicular to the surface of the radiator in the limit of small final spot size. This property of the design is illustrated in Figure 6, a cross section through the counter showing the $\pm 5^\circ$ particle trajectories. Also shown are some Cerenkov light rays. Note that, with the curved surface, the light from the back of the cell emerges at a steeper angle than the light from the front. This property improves the probability of light being collected as shown in Figure 6. The six phototubes used in this counter are RCA type 8851. This tube has a first dynode of gallium phosphide and a voltage drop between the cathode and first dynode of 600 volts. The electron amplification of this first stage is between 30 and 50 and the width of the Poisson distribution is such that it is possible to discriminate between pulse heights resulting from one photoelectron, two photoelectrons, three photoelectrons, etc. Since the dark current consists of single photoelectrons, the background if two or more photoelectrons are required is very low. It was found that requiring all six tubes in coincidence gave poor efficiency, and in some of the running, a voter coincidence was used. A voter coincidence gives an output pulse if more than n input pulses appear simultaneously at the input ($n \leq 6$); the value of n is determined by a selector switch. Because an unwanted particle can go through the counter on an angle and trigger all the tubes on one side, it is believed that arrangements that require tubes on opposite sides to trigger combine good efficiency with good rejection in a more efficient way. Some possible coincidence arrangements are shown in Figure 7. These arrangements have an efficiency comparable to requiring four out of six on the voter coincidence, but should give better rejection of a scattered pion.

The theoretical efficiency of this counter can be calculated given two things: the average number of photoelectrons produced in each tube by a real event and the triggering mode. If use is made of the special properties of the cell so that two or more photoelectrons are required to produce a discriminator pulse, then the probability P, that a trigger will result is given by

of the 8851 tube so that k or more photoelectrons are required to produce a discriminator pulse, then the probability, P , that a trigger will result is given by Poisson statistics

$$(9) \quad P(\geq k) = 1 - e^{-n} \sum_{i=0}^{k-1} n^i / i!$$

The efficiency for a 6 fold coincidence is P^6 . Some other efficiencies are given in Table II.

TABLE II

5 out of 6 vote	$P^6 + 6 P^5 (1-P)$
4 out of 6 vote	$P^6 + 6P^5 (1-P) + (6 \cdot 5/2!) P^4 (1-P)^2$
Two pair (Fig. 7a)	$P^6 + 3P^4 (1-P)^2$
Triples (Fig. 7b)	$1 - (1-P^3)^2 = 2P^3 - P^6$
Three ORs (Fig. 7c)	$(2P - P^2)^3$

The expected efficiency of the counter as a function of n , the average number of photoelectrons/tube is shown in Figure 8 for $k=1$ and 2 and various triggering requirements. A rough estimate of n might be to divide the number of photoelectrons in Figures 3 and 4 by 6, however, the efficiency calculated this way is much higher than that actually obtained; it appears that Figure 3 grossly overestimates the collection efficiency. Instead Figure 8 may be used to determine n given the measured efficiency and triggering mode.

Test of Efficiency With Protons

If two Cerenkov counters are available the efficiency and rejection of each can be obtained directly. Since only one of these counters has been built, an indirect method of testing had to be used to find the optimum voltage settings on the tubes and to determine efficiency and rejection. A test was set up in the low energy (-19°) beam from G10. Tuned to positives at 1.5 GeV/c, this beam has about equal numbers of π^+ and protons. The protons can be cleanly separated from the pions (and K's) by time-of-flight technique and have about the same β as 800 MeV/c K's. The electronics of the test setup is shown in Figure 9. The composition of the beam was determined by a toggle switch delay box; a change of 8nsec could switch the beam from ~100% pions to ~100% protons.

The tube gains were initially balanced using an Am²⁴¹ α source attached to a piece of plastic scintillator. The voltage input to the power divider was then varied to find a level that combines the best rejection with good efficiency. Some data taken in the test beam is shown in Table III.

TABLE III

Coincidence Requirement	Timing Set for π 's			Timing Set for Protons		
	S	SC	SC/S	S	SC	SC/S
Vote ≥ 2	316	10688	2.9%	10505	10618	99.2%
≥ 3	133	10177	1.3%	10074	10218	98.6%
≥ 4	17	10987	.15%	10172	10944	92.9
≥ 5	46	105119	.044%	8294	11009	75.3
≥ 6	5	101155	.005%	2447	10089	24.2%
1 Pair	91	10286	.88%	10033	10340	97.0%
2 Pairs	11	10669	.10%	10024	11297	88.9%

From the fact that the pion rejection with 6 out of 6 required is very high, while the proton efficiency with 2 out of 6 is almost 100% it can be seen that the time-of-flight selection was able to produce a very clean separation. The best compromise appears to be 4 out of 6. A later test with the tube voltages adjusted somewhat differently gave a rejection of .06% and an efficiency of 94.1%.

Operation in LESB

It is not safe to assume that this efficiency and rejection can be duplicated in the LESB where the beam is less parallel and the counting rate is much higher. It has been possible to establish that the rejection is sufficiently good by means of time-of-flight measurements. Figure 10 shows a Polaroid picture of a time-of-flight spectrum taken with a EG+G time-to-amplitude converter and a 100 channel PHA. To get good resolution the second counter had to be placed about 15 ft. behind the experimental focus; this path length would not be available for the actual experiment where the K's would be stopped. The top trace, ungated, shows peaks for π 's, K's and protons. The bottom trace, which was gated by the Cerenkov counter, shows only the K peak. Clearly anything identified by this counter as a Kaon is pretty likely a Kaon.

Figure 10 was taken at the K peak of the separator curve, where the singles counting rates are moderate. Under the pion peak, rates are ~ 100

times larger, and there is a considerable number of spurious counts. Figure 10 was taken with a ≥ 4 coincidence requirement. Since then it has been found that the 3 OR mode, Figure 7c, while giving the same or better counting rate under the K peak gives better rejection under the pion peak. The absolute efficiency in the LESB cannot be determined until two counters are available. A second counter is now under construction.

Acknowledgments

The author wishes to thank M. Koson and D. Salimando for their work in construction of this counter. He would also like to thank the Princeton Group (G. Sanders, C. Hoffman, and S. Smith) for several suggestions relating to the testing of this counter and for the loan of an 8575 tube as a temporary replacement for one of the 8851's that went bad.

References

- (1) B.A. Leontic and J. Teiger BNL 50031 (1966)
- (2) S. Ozaki et al Nucl. Instr. & Meth. 35 301 (1965)
- (3) V. Fitch and R. Motley Phys. Rev. 101 496 (1956)
- (4) J. Seguinot et al Nucl. Instr. & Meth. 10 205 (1961)
- (5) e.g. Panofsky & Phillips Classical Electricity and Magnetism (Addison Wesley 1955) pp. 312
- (6) Pilot Chemical Co. 36 Pleasant St., Watertown, Mass. 02172

PARTIAL LIGHT COLLECTION EFFICIENCY

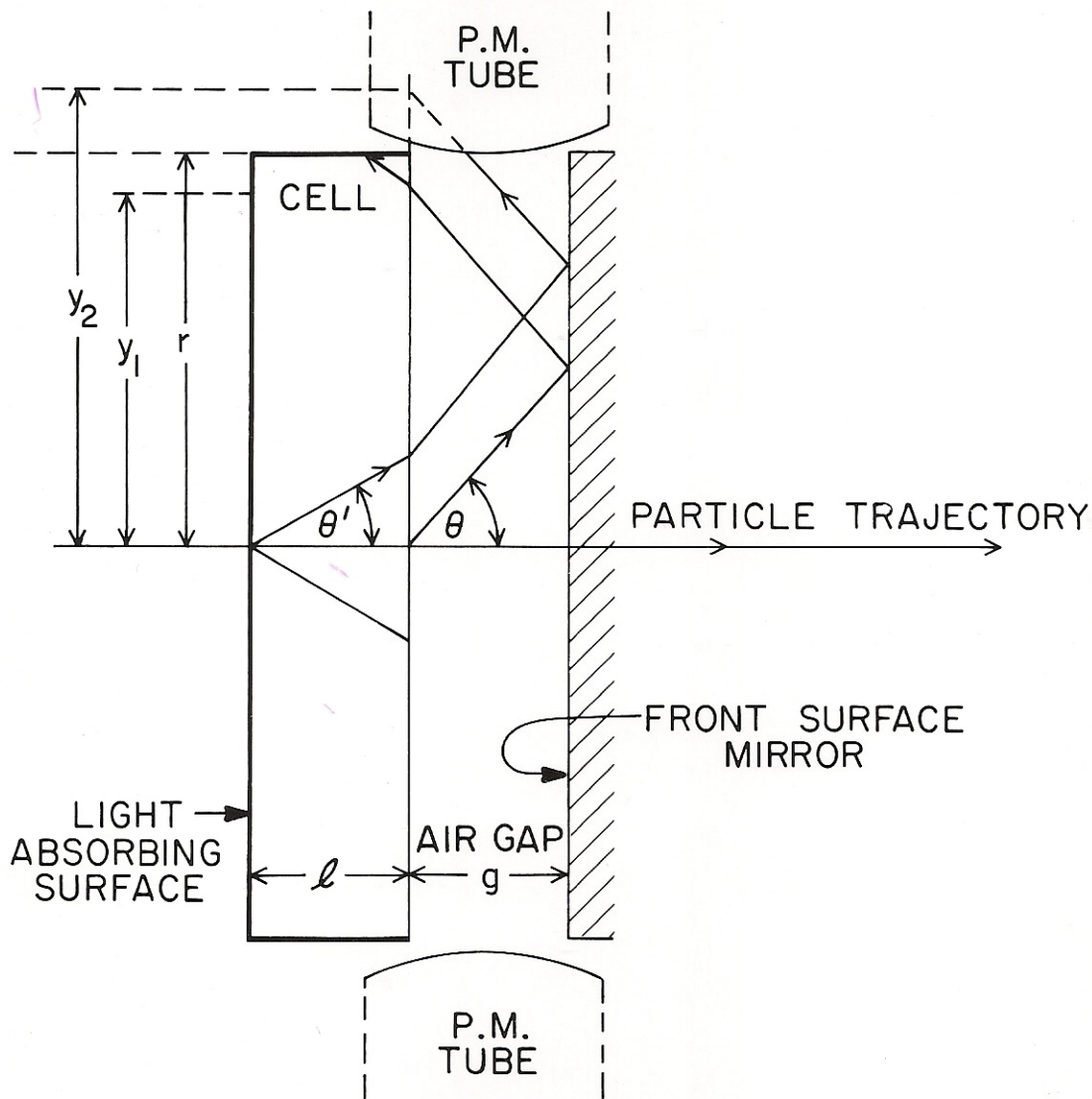


Fig. 1

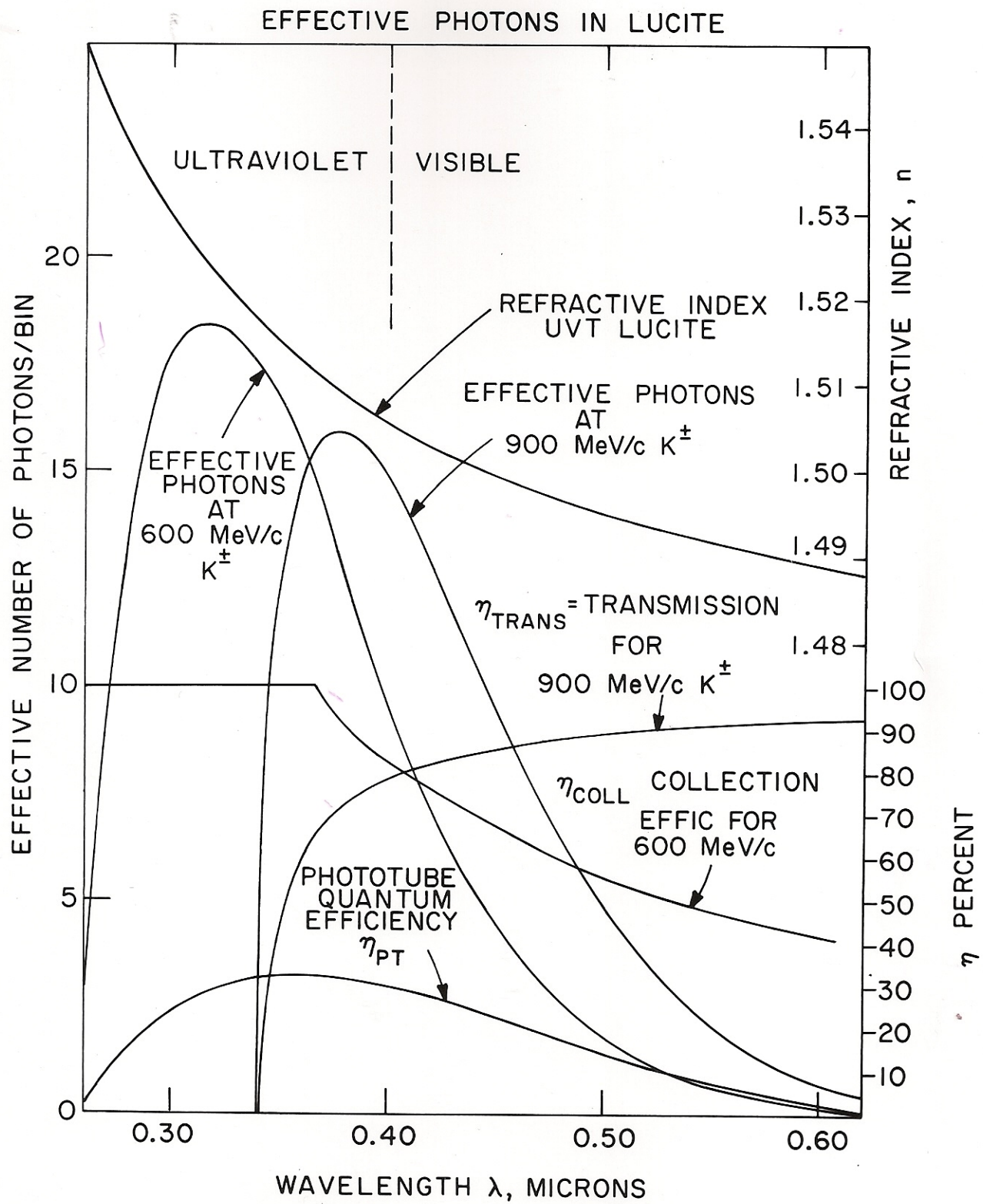


Fig. 2

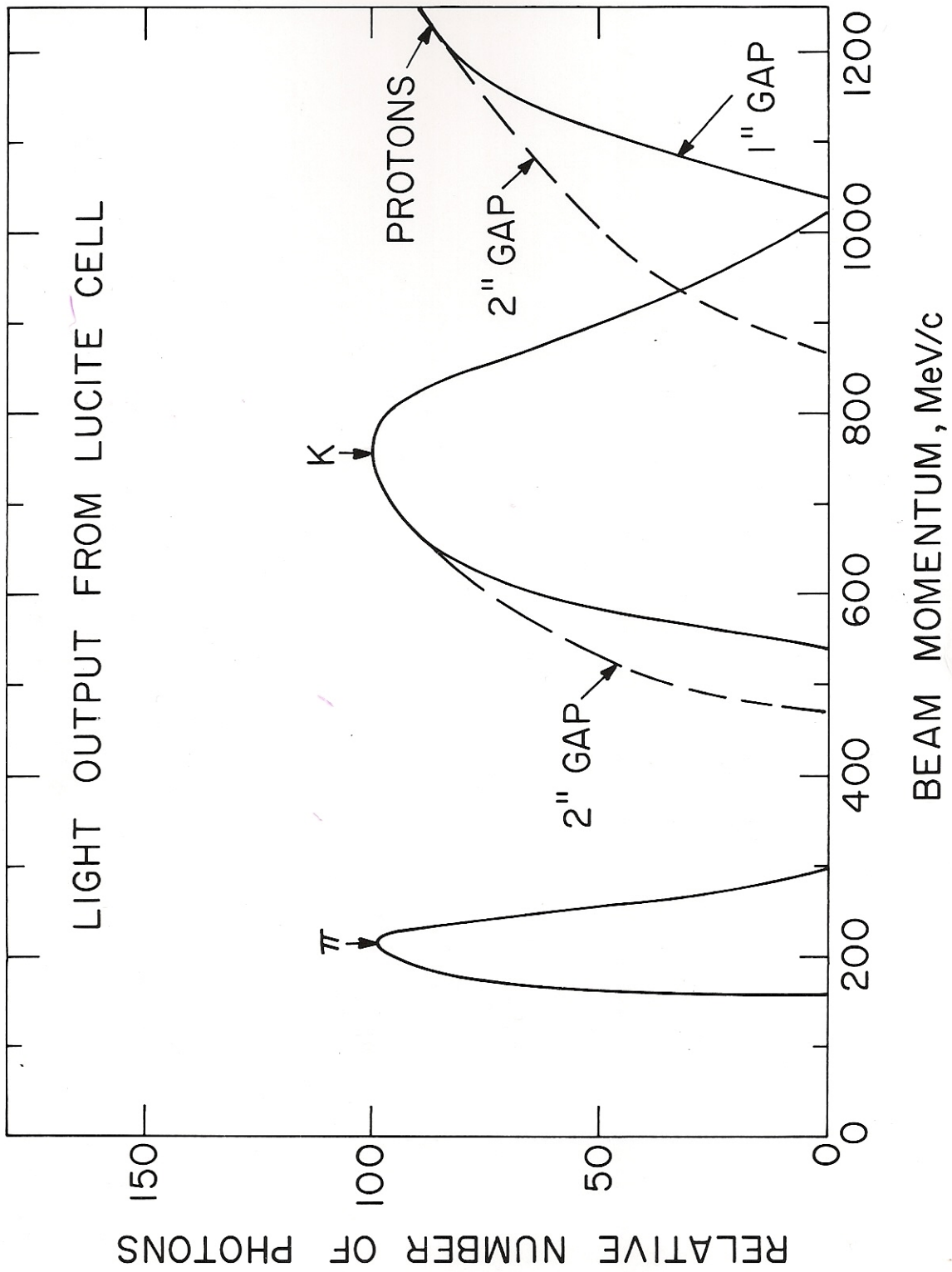


Fig. 3

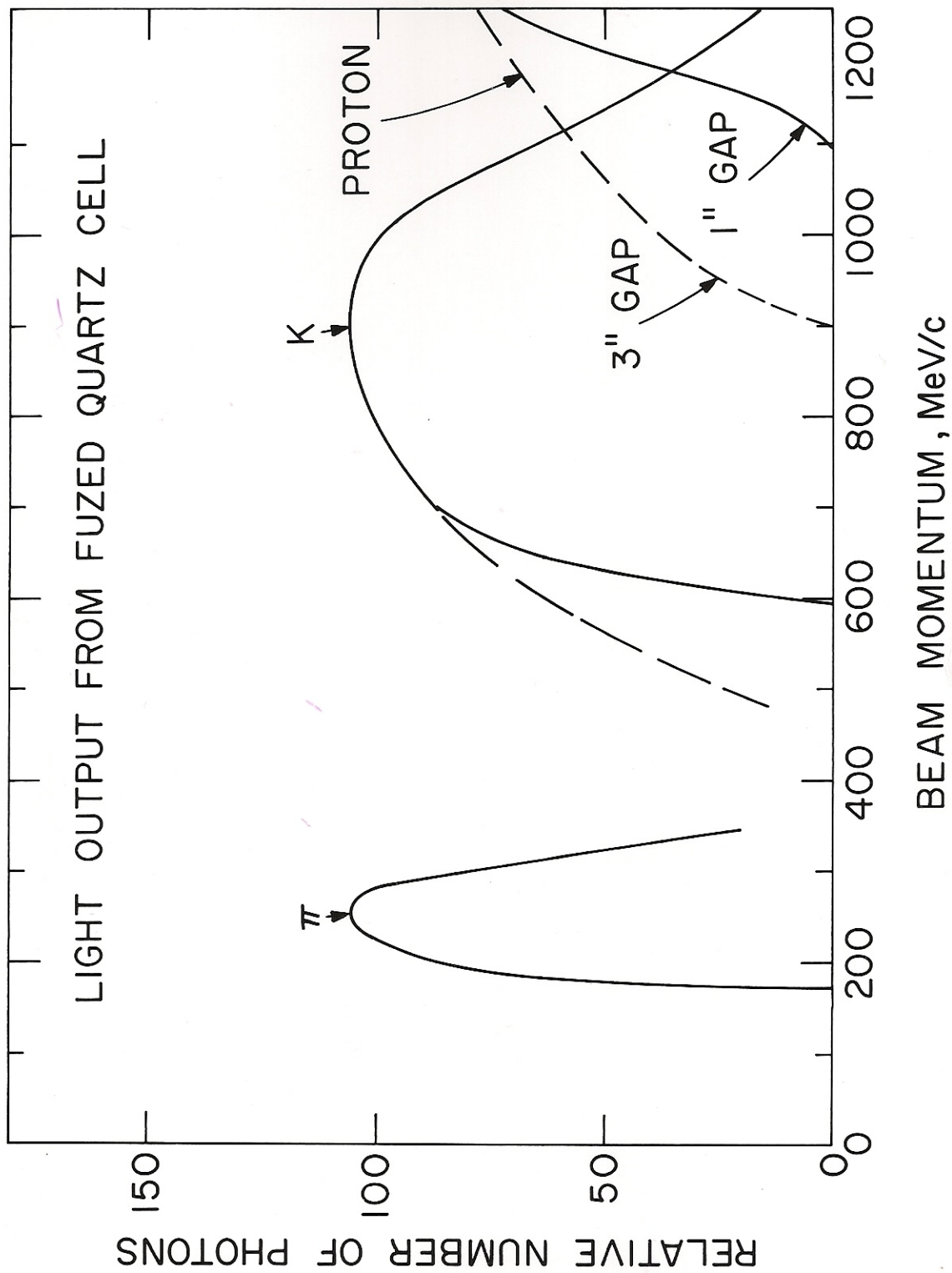


Fig. 4

BOX FOR DIFFERENTIAL ČERENKOV COUNTER

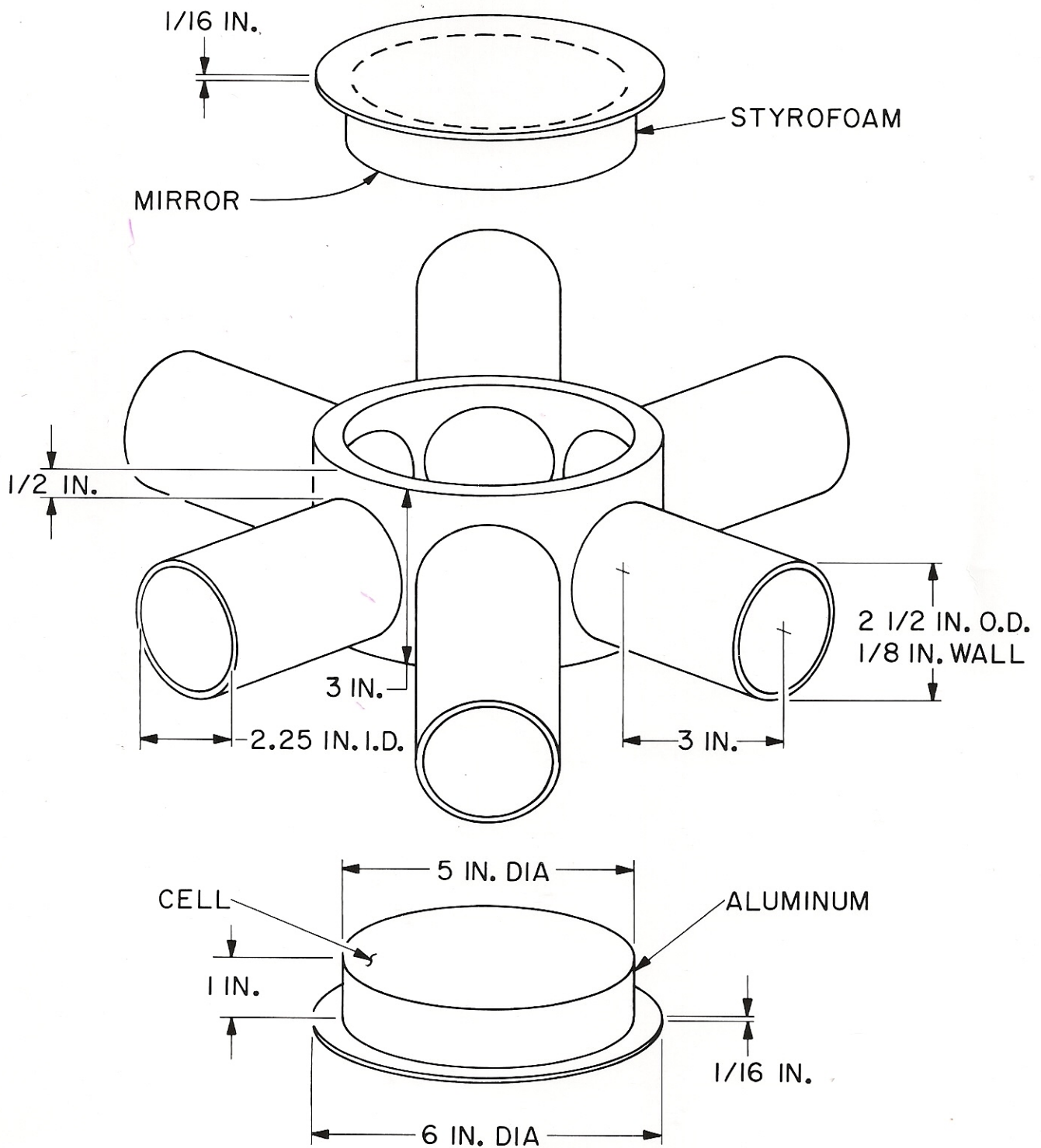


Fig. 5

RAY TRAJECTORIES FROM CURVED RADIATOR

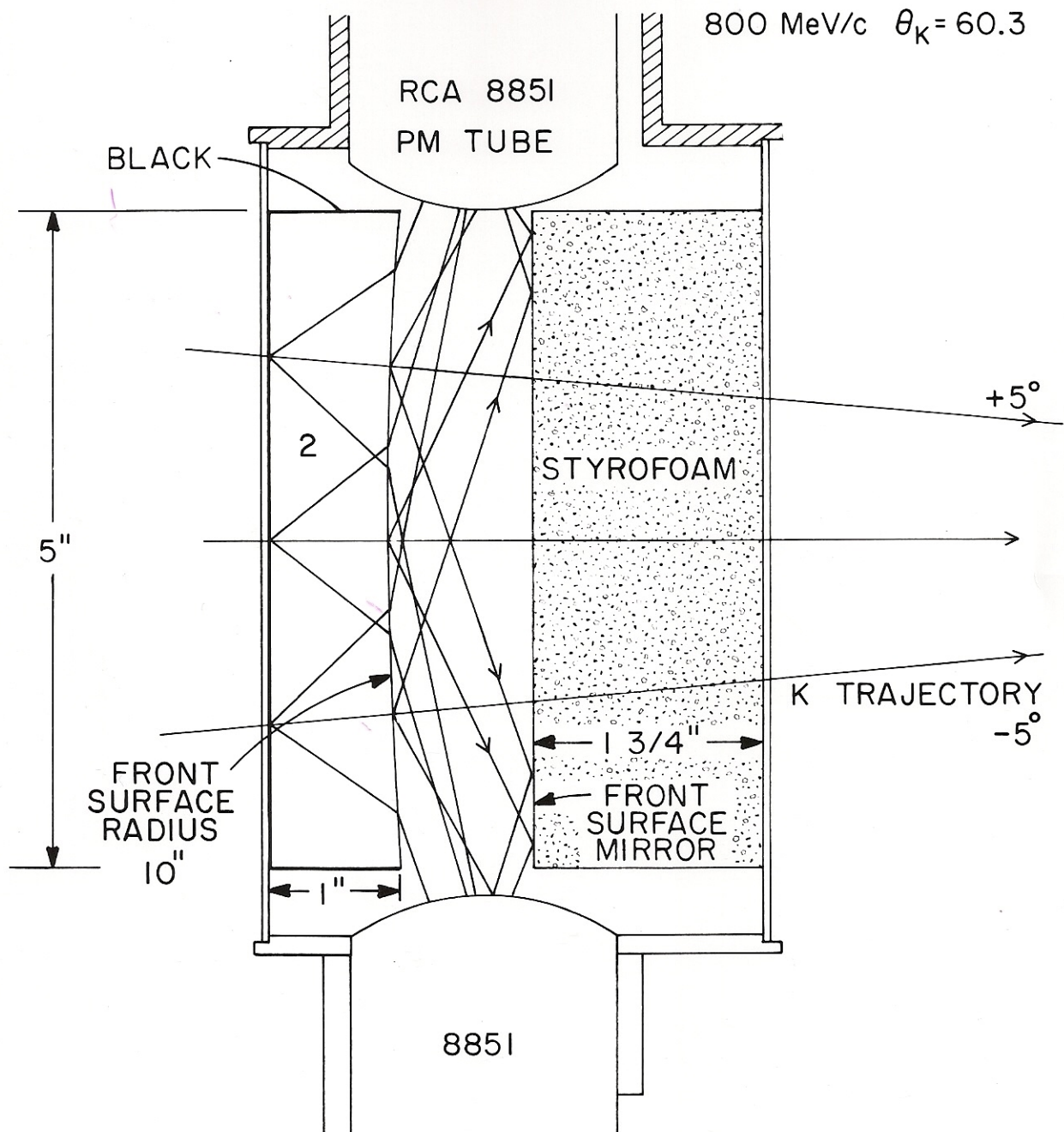
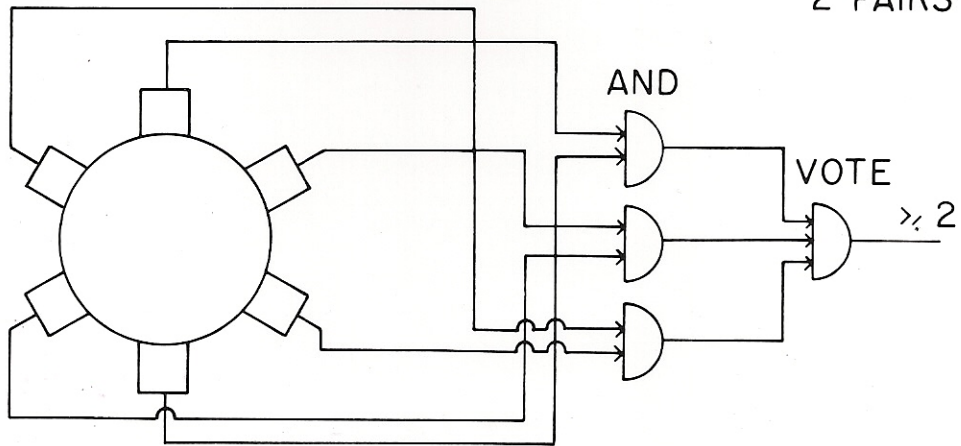


Fig. 6

TRIGGERING MODES

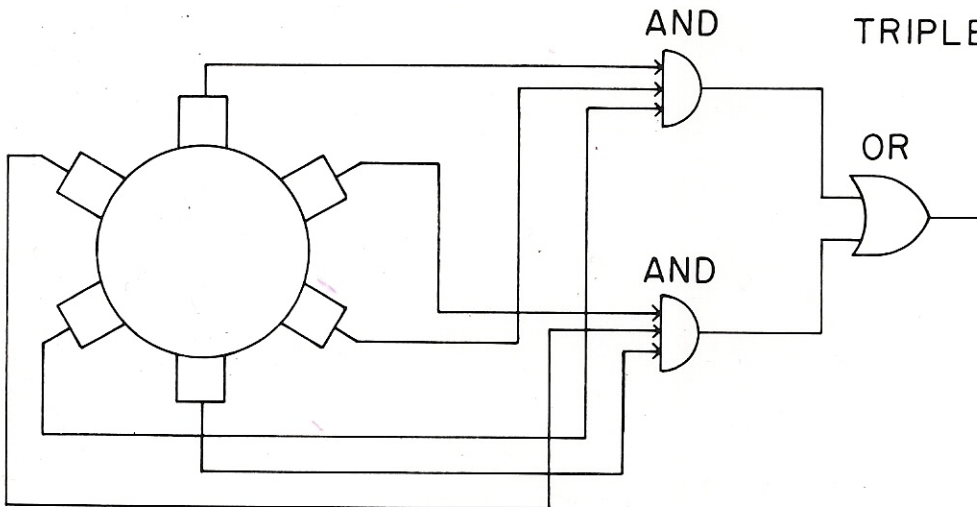
2 PAIRS

7a



TRIPLETS

7b



TRIPLE OR

7c

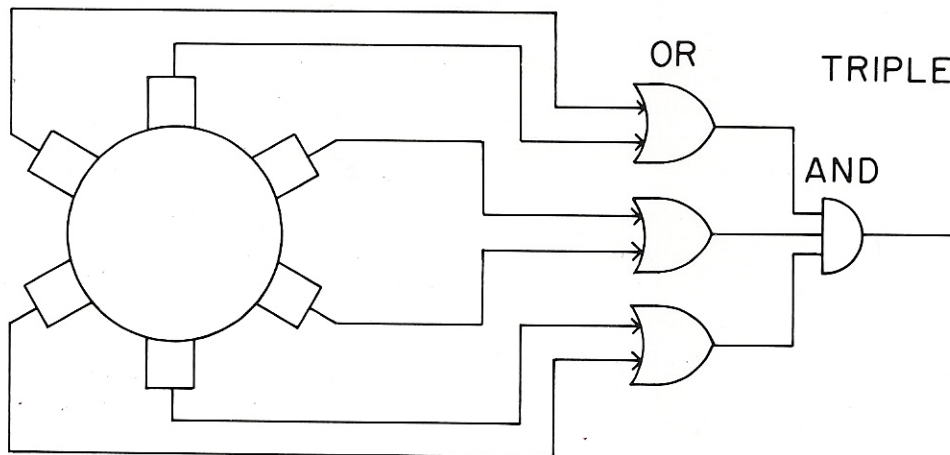


Fig. 7

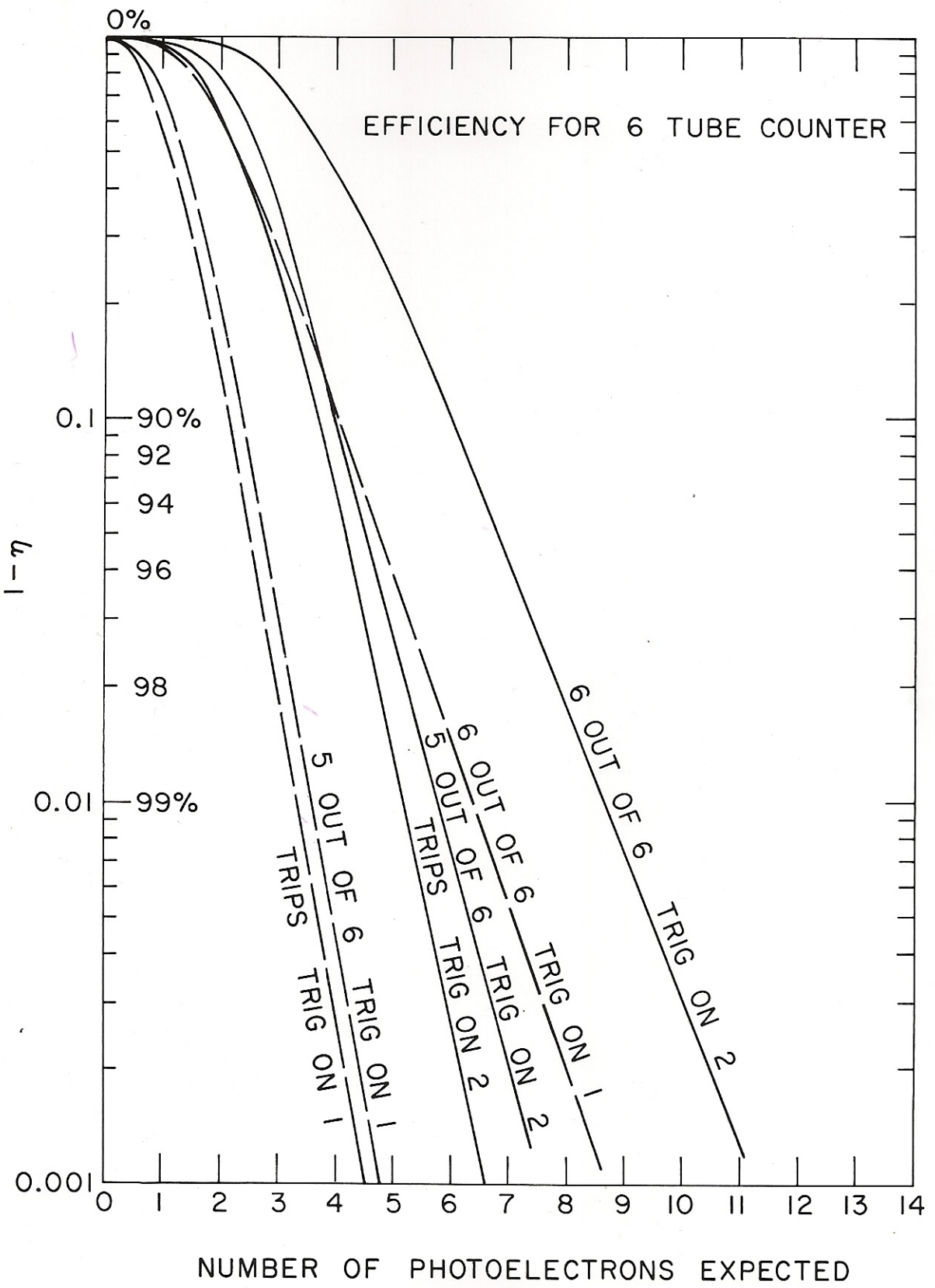


Fig. 8

TEST BEAM SETUP

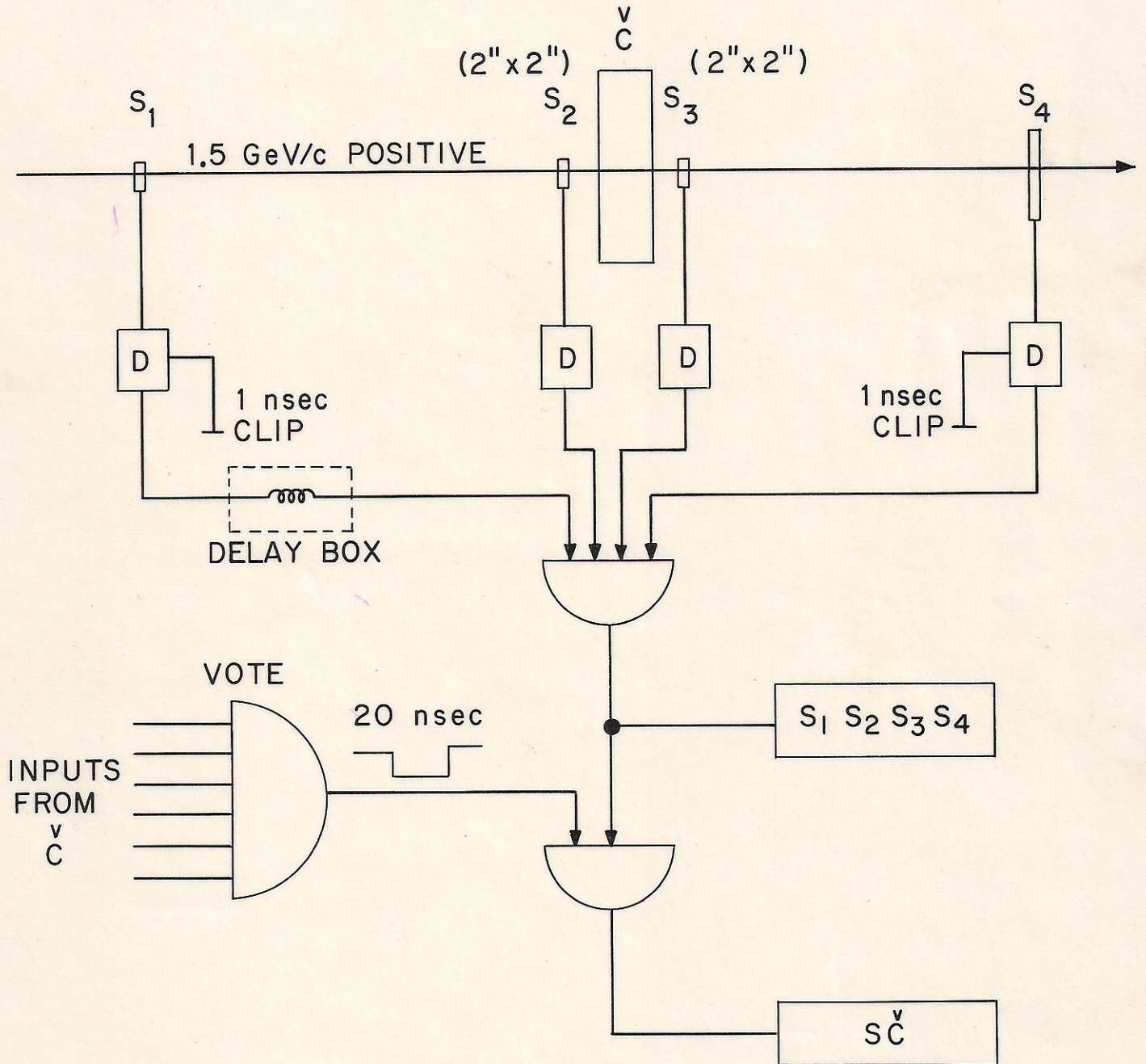


Fig. 9

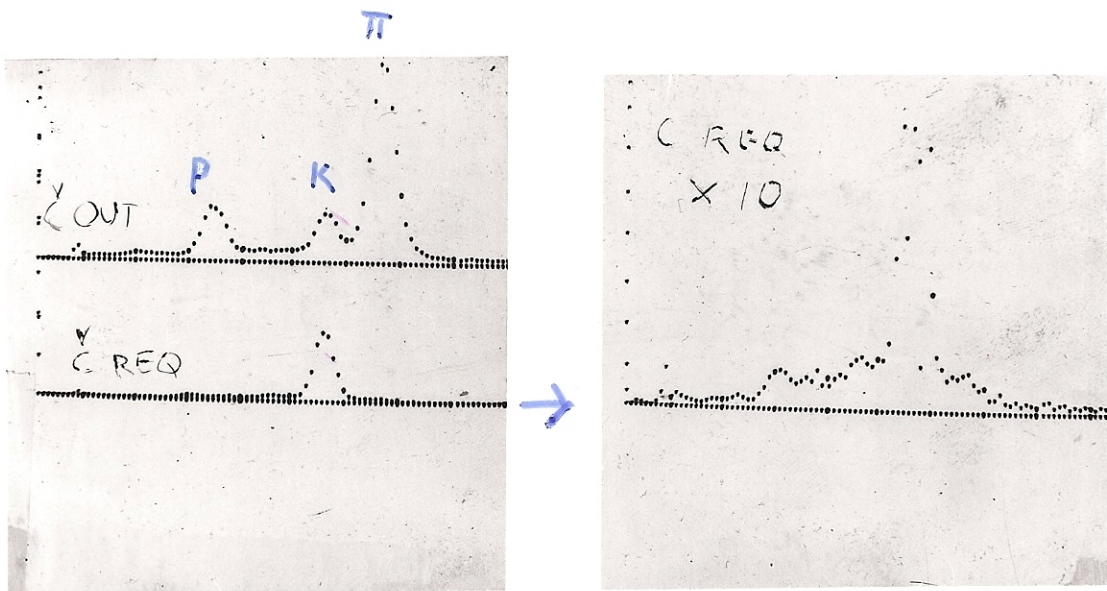


Fig. 10